

General Disclaimer

One or more of the Following Statements may affect this Document

- This document has been reproduced from the best copy furnished by the organizational source. It is being released in the interest of making available as much information as possible.
- This document may contain data, which exceeds the sheet parameters. It was furnished in this condition by the organizational source and is the best copy available.
- This document may contain tone-on-tone or color graphs, charts and/or pictures, which have been reproduced in black and white.
- This document is paginated as submitted by the original source.
- Portions of this document are not fully legible due to the historical nature of some of the material. However, it is the best reproduction available from the original submission.

X-621-69-130

PREPRINT

NASA TM X-63613

**SOME IONOSPHERIC PROPERTIES
AT 1000 KILOMETERS ALTITUDE WITHIN
THE AURORAL OVAL**

**P. L. DYSON
A. J. ZMUDA**

APRIL 1969



**GODDARD SPACE FLIGHT CENTER
GREENBELT, MARYLAND**

N69-33441

(ACCESSION NUMBER)		(THRU)	
47		1	
(PAGES)		(CODE)	
1		13	
(NASA CR OR TMX OR AD NUMBER)			
TMX-63613			
(CATEGORY)			

FACILITY FORM 602

X-621-69-130
PREPRINT

SOME IONOSPHERIC PROPERTIES AT 1000 KILOMETERS
ALTITUDE WITHIN THE AURORAL OVAL

P. L. Dyson

Aeronomy Branch

Goddard Space Flight Center

Greenbelt, Maryland

and

A. J. Zmuda

Applied Physics Laboratory

Johns Hopkins University

Silver Spring, Maryland

Goddard Space Flight Center

Greenbelt, Maryland

PRECEDING PAGE BLANK NOT FILMED.

CONTENTS

	<u>Page</u>
ABSTRACT	iv
1. INTRODUCTION	1
2. THE EXPERIMENTS	2
3. PRESENTATION AND DISCUSSION OF RESULTS	5
The data	5
Latitudinal variations in T_e and N_e	6
Fluxes	11
Comparison of Results with Other Experimental Observations	12
4. INTERPRETATION	14
Effects of Precipitating Particles	14
Effect of Field-Aligned Currents	16
T_e Within the Oval	17
5. CONCLUSIONS	19
APPENDIX – Effect of Particle Fluxes on Probe Current	21
ACKNOWLEDGMENTS	23
REFERENCES	25

SOME IONOSPHERIC PROPERTIES AT 1000 KILOMETERS ALTITUDE WITHIN THE AURORAL OVAL

P. L. Dyson* and A. J. Zmuda

ABSTRACT

Explorer 22 electrostatic probe measurements of electron density (N_e) and temperature (T_e) show that at 1000 km altitude the ionosphere within and near the auroral oval is characterized by relatively large latitudinal variations in both N_e and T_e . Electron density enhancements occur which vary from the order of ten kilometers to several hundred kilometers in horizontal extent. They vary in magnitude from increases of 10% upwards and the N_e enhancements are larger at night. Smaller scale variations (~ 1 km) also occur in N_e . The degree of correlation between T_e and N_e varies because of the dynamic nature of the phenomena occurring in the oval region. Simultaneous measurements of local magnetic field fluctuations in the oval show that often the ionosphere is most irregular in the region where the magnetic disturbances occur. It is likely that the magnetic disturbances are the result of field aligned currents but the direct ionospheric effects of such currents are too small to cause the changes observed in N_e and T_e . Often the maximum values of T_e in the oval appear too high to result from energetic auroral bombardment alone and it is likely that either low energy electrons (~ 5 ev) constitute a significant heat source at 1000 km in the auroral oval or that there is a heat source in the outer magnetosphere and that the high temperatures result from thermal conduction.

*NRC-NASA Resident Research Associate.

SOME IONOSPHERIC PROPERTIES AT 1000 KILOMETERS ALTITUDE WITHIN THE AURORAL OVAL

1. INTRODUCTION

A narrow, closed, high-latitude region exists where large geophysical disturbances occur at all longitudes along what is called the auroral oval [Akasofu, 1966] because of its oval shape (centered roughly at the dipole pole) and its association with the spatial distribution of visible aurora [Feldstein, 1963, 1966; Akasofu and Chapman, 1963; Piddington, 1965; Akasofu, 1966]. The auroral oval also marks the magnetic shells near or coincident with those containing the following phenomena which are often treated in terms of a diurnal variation: the polar electrojet [Akasofu et al., 1965; Feldstein, 1966]; the outer boundary of trapped electrons [O'Brien, 1963; McDiarmid and Burrows, 1964; Frank et al., 1964; Williams and Palmer, 1965; Williams and Mead, 1965]; the maximum electron precipitation [O'Brien, 1962; McDiarmid and Burrows, 1964; Frank et al., 1964]; the region with the radio aurora, also shown to match that of the visible aurora [Bates, 1966; Bates et al., 1966]; and large, transverse magnetic disturbances at 1100-km altitude [Zmuda et al., 1966, 1967; Heuring et al., 1968] which Cummings and Dessler [1967] relate to field-aligned currents. Theoretical models potentially applicable to the currents and fields in the oval have been reviewed by Boström [1967], Schield [1968] and Schield et al., [1969].

Recent studies of the topside ionosphere in the auroral and polar regions show that a number of maxima and minima occur in the latitudinal variation of

electron density. The most prominent and widely studied of the maxima is the "polar peak" which is several hundred kilometers wide, occurs on the dayside and is most pronounced near magnetic noon (Thomas et al., 1966; Nishida, 1967; Donley, 1968). Large latitudinal variations in the ion density have also been observed in the polar region near 1000 km altitude (Taylor et al., 1968). Electron density fluctuations with smaller horizontal scales (1 to 10 km) also occur in the topside auroral ionosphere (Calvert and Van Zandt, 1966; Lund et al., 1967). The density in these irregularities varies from the ambient by up to a factor of 5 and Lund et al. (1967) found that irregularities with large amplitudes were associated with auroral precipitation.

The Explorer 22 satellite (1964, 64A) which was launched into a nearly circular orbit at 1000 km with an inclination of 80° , offers an opportunity to study the auroral ionosphere as it contains an electrostatic probe experiment for measuring density (N_e) and temperature (T_e) and a Schonstedt fluxgate magnetometer to detect the variations marking the auroral oval field lines. In this paper we present the results of simultaneous observations made by these experiments at high latitudes and in the auroral oval. The observations were made between April 26 and August 30, 1967 at the Applied Physics Laboratory's tracking station in Maryland.

2. THE EXPERIMENTS

Explorer 22 is magnetically stabilized and contains two electrostatic probes mounted so that one probe is parallel to the magnetic field and the other is anti-parallel. Details of the probe experiment have been given elsewhere by Brace

and Reddy (1965a, b) and Brace et al. (1967, 1968) who also discussed properties of the low and mid-latitude ionosphere at 1000 km; but those aspects important to this study will be repeated here. The data presented were obtained when the probe experiment was operated in a "continuous mode" (Findlay et al., 1969) which enables the N_e and T_e structure to be studied in more detail than when the normal operating mode is used.

A 2 Hz sawtooth voltage is applied first to one probe and then to the other, alternating every 2.6 seconds and the resulting probe currents are telemetered to the ground. The voltage is swept from -3 to +5 volts with respect to the satellite. Typical volt-ampere characteristics are shown in Figure 1. T_e and N_e are determined from the electron retardation and saturation regions respectively (Mott-Smith and Langmuir, 1926; Spencer et al., 1965). The current detector has two ranges which are alternated every 5.5 seconds. T_e can generally be measured on both current ranges although the values determined from the low current range are more accurate because the resolution in the retardation region of the volt-ampere curve is better. For the low current range the absolute accuracy is believed to be better than 10% and the relative accuracy 5%. In the high current range, accuracy decreases by less than a factor of two. Generally N_e can only be calculated from the high-current range but this data can be supplemented by using the ion current data. The stationary probe theory is not strictly valid in the ion saturation region because the ion thermal velocity (particularly of the major constituent at high latitudes, O^+) is less than the satellite

velocity. However the ion current (i_I) remains proportional to the ion density (Brace et al., 1965). The relative accuracy of the N_e measurements is about 5% and the absolute accuracy about 20%. The relative accuracy of the ion current is better than 5% for the more sensitive current range.

Since one volt-ampere curve is obtained in 0.5 seconds and the satellite velocity is about 7 km/sec, values of T_e and N_e are obtained at approximately 4 km intervals along the satellite path. The measurements are interrupted at regular intervals by in-flight calibrations of the experiment. Thus variations in T_e and N_e with horizontal scales of the order of 10 km and larger can be readily detected. At middle and high latitudes the probes are not seriously waked except when they pass behind a solar paddle and these effects are easily recognized and distinguished from ionospheric variations. If N_e irregularities of 10% or more with horizontal scales of about 1 km or less are present these can also be detected as they will cause distortions in individual volt-ampere characteristics (Brace and Reddy, 1965b; Dyson, 1969).

The magnetometer is oriented so that it detects magnetic field variations in the plane perpendicular to the field direction. Further description of this instrument is given by Zmuda et al. (1966, 1967).

3. PRESENTATION AND DISCUSSION OF RESULTS

The Data:

The data presented here were received at the tracking station in Maryland operated by the Applied Physics Laboratory (APL) of Johns Hopkins University. Data were obtained from within the region bounded by 30°N and 80°N contours of invariant latitude ($\cos \Lambda = (1/L)^{1/2}$) and the 55°W and 95°W geographic meridians. Data from 63 continuous mode passes were employed in this study. During the period under study here, the satellite potential was unusually high and for most of the passes only the variations in i_I could be measured. Although i_I results largely from the thermal ions in the plasma, it also has components due to photoionization and particle fluxes and changes in i_I may be due to changes in any of these. For passes in which both i_I and N_e could be measured, the variations in N_e and i_I along the satellite path were compared to determine the extent to which changes in i_I occurred that were not the result of variations in the ion density. Good agreement between changes in N_e and i_I , and hence negligible contributions due to photo-ionization and particle fluxes were found particularly at low latitudes where the latitudinal gradients of ionospheric properties are relatively small. This is true also at high latitudes if variations in i_I with horizontal dimensions less than about 25 km were ignored; sample plots are shown in Figures 2a, 2b, and 2c. This spatial resolution, which can be lowered to about 10 km in special cases, represents a considerable improvement over earlier ionospheric work but unfortunately restricts detailed comparisons

with the magnetic variations. Reasons for this limit will be discussed later. In this paper we are concerned primarily with the variability of the electron density along the satellite path and it is considered that whenever N_e is not directly determinable then large changes in the variability can be found from i_I if variations less than 25 km in extent are ignored. The eleven passes for which N_e and i_I could be measured were used to obtain an empirical linear relationship between i_I and N_e . The resulting expression is accurate to within 20%, the error being approximately constant throughout each pass.

Latitudinal variations in N_e and T_e .

Figure 2 shows N_e measured along the satellite path for three passes. With respect to Figure 2a as an example, in the region up to 60° invariant latitude N_e varies slowly in a manner similar to that reported by Brace et. al. (1967) for the same local time and season during 1965. The main difference is the overall increase in N_e caused by the increase in solar activity (Brace et. al., 1968). However, above 60° the N_e latitudinal gradient increases markedly and a number of maxima and minima occur.

Although the latitudinal variation of electron density within the auroral oval is often different from one pass to the next a characteristic pattern tends to occur near the equatorward edge of the oval, particularly at nighttime. In these cases the equatorward boundary is marked by a relatively large increase in N_e . Moving towards the pole, N_e first decreases and then increases following a well

defined minimum in which N_e is often close to or less than the value just equatorward of the irregular region. Further poleward, N_e fluctuates but the peaks and valleys are not as pronounced. An example of this type of variation is shown in Figure 2(a). Small scale irregularities of the order of a kilometer were also observed in the oval region.

Figure 2 also shows the latitudinal variations in T_e and it is apparent that T_e is most variable in the region where N_e fluctuates. Magnetic disturbances were also observed in the region of the large T_e and N_e variations suggesting that the latter is related to the auroral oval. For passes occurring on magnetically quiet days ($K_p \leq 2+$) the logarithmic N_e gradient.

$$\left(\frac{1}{N_e} \frac{dN_e}{dx} \right), \text{ km}^{-1}$$

Along the satellite path has been measured at several latitudes and plotted as a function of invariant latitude for night time (2000 - 2400 LT) and daytime (0900-1300) passes, (Figure 3). At mid-latitudes the gradient is generally less during the day than at night a result which agrees with that of Brace et al. (1968). At high latitudes the gradient is much more variable and is typically a factor of 10 greater than at mid-latitudes. There is also a diurnal variation at high latitudes in that during the daytime the maximum gradients occur at latitudes higher than those for the nighttime. The daytime and nighttime locations of the auroral oval are also marked in Figure 3, there representing the composite derived from the

magnetic disturbances for the individual passes. It is evident that the maximum gradients occur either in or equatorwards of the oval. At night the region of large N_e gradients occurs poleward of the minimum of the electron density trough reported by Muldrew (1965) and others. The data reported here were obtained during local summer where the trough is not very pronounced (Nishida, 1967) and some nighttime passes showed very little evidence of a trough at all.

In most cases when an irregular region was observed in the ionosphere the satellite was still in this region as it passed below the poleward horizon of the tracking station. There were several nighttime cases, however, in which a poleward boundary of the irregular ionosphere was observed. Poleward of this boundary the electron density gradients generally decreased.

A more complete picture of the diurnal behaviour of the position of the irregular ionosphere is given in Figure 4 which shows the average location of the equatorward boundary of the irregular ionosphere as a function of local time for different values of K_p . Similar plots are also shown for the equatorward boundary of the transverse magnetic disturbances.

For the quiet period, the invariant latitude of the magnetic disturbance boundary is between 74° and 77° in the period 1000 - 1300 LT and about 68° around local midnight. As the magnetic activity increases, the disturbances move equatorward. These characteristics are similar to those observed with satellite 1963 38C (Zmuda et al., 1966, 1967; Heuring et al., 1968). The behaviour of the irregular ionosphere with both local time and K_p is very similar

to that of the magnetic disturbances except that the irregularities begin equatorward of the magnetic disturbances. Ionospheric irregularities always appeared in the region containing the magnetic disturbances so that they also are a feature of the auroral oval.

The difference in the locations of the equatorward boundary of the irregular ionosphere and the magnetic disturbance region could be due to instrumental effects because the threshold level of the magnetometer is $\sim 30 \gamma$ and it measures only one component of the disturbance in the plane transverse to the field direction. Another factor is that since the auroral oval position varies with time, the ionospheric irregularity outside the instantaneous oval position may be the residue of an irregularity produced at an earlier time by the oval phenomena. Significant variations in the magnetic disturbance amplitude occur over distances smaller than the resolution of the N_e measurements so that detailed comparisons between the magnetometer and N_e variations are not possible. Comparisons on a gross scale indicate that in over 50% of the passes in which magnetic disturbances were observed, the ionosphere was most irregular in the magnetic disturbance, or ΔB , region (Table 1). The magnitudes of the irregular features apparently do not depend on whether or not they occur in the magnetic disturbance region (Table 2). However, this result may also be at least partly due to the limitations in the magnetometer sensitivity and the dynamic nature of the disturbance. Further evidence of the relation between these auroral phenomenon was obtained with the same experiment by Findlay et al. (1968) who found that during

the large magnetic storm of May 26, 1967, visual aurora were observed in the same regions in which the ionosphere was irregular and in which transverse magnetic disturbances occurred.

Figure 5 consists of histograms showing the ratio of the maximum and minimum values of electron density (N_{\max} and N_{\min} respectively) in the oval region and the poleward density (N_p) to the equatorwards (N_{eq}) of the oval. It is evident that the maximum values in the oval are typically 20% higher than the equatorward values while the minimum values are about the same as those equatorward of the oval. Poleward of the oval the density is less than the maximum oval value but may be greater than or less than both the oval minimum value and the values equatorward. Figure 6 shows the magnitude and horizontal extent of the electron density enhancements which exceed 0.5° in latitudinal width. Here the magnitude of the enhancement is defined as

$$\frac{N_{\max} - N_{\min}}{N_{\min}} \times 100 \%$$

At night (solar zenith angle $\chi \geq 100^\circ$) most of the enhancements were more than 20% in magnitude and were larger than those of the daytime ($\chi \leq 80^\circ$) which were nearly all less than 30% in magnitude. There is no significant diurnal change in the horizontal extent of the peaks.

T_e could be measured during only a small number of passes which are listed in Table 3. The maximum and minimum T_e values in the irregular ionosphere, the value of T_e outside this region and the latitudinal T_e gradients are tabulated.

T_e equatorwards of the irregular ionosphere could not always be measured so that in some cases the background T_e value was measured on the poleward side. It is evident that T_e behaves similarly to N_e in that higher values occur in the irregular region and the latitudinal gradients are also larger.

To summarize, the irregular ionosphere is a region characterized by steep gradients in N_e and T_e and a number of maxima and minima with peak values generally higher than in the ionosphere immediately equatorwards and polewards.

Fluxes

It was pointed out earlier that the variations in i_I and N_e are not always in agreement over distances of 25 km or less. In some of these cases a change in i_I occurs when there is no change in N_e , as at 0401:32 UT in the data shown in Figure 7. These changes have been attributed to fluxes of particles of sufficiently large energy that their collection is unaffected by the voltage applied to the probe, -3 to +5 volts. By making certain assumptions it is possible to estimate the magnitude of the fluxes (see Appendix): The i_I -change shown in this figure is consistent with effects due to either a proton flux of $\sim 10^{10}$ particles/cm² sec ster or an electron flux of $\sim 5 \times 10^{10}$ particles/cm² sec ster in the energy range 0.1-1.8 kev with both flux values being reasonable for auroral particles. The flux either persisted for about two seconds or had a north-south extent of about 10 kilometers.

Particle counter measurements indicate that the proton flux above 10 kev is $\sim 10^7$ particles/cm² sec ster but it is likely that the flux below 10 kev may exceed

that above by a factor of 100 (Eather, 1967). Hence low energy proton fluxes could be responsible for the observations although as yet there are no particle detector observations of such intense proton fluxes with either such small latitudinal dimensions or short time durations.

In the case of electron fluxes, intensities of $\sim 10^{10}$ electrons/cm² sec ster at energies below 2 kev are known to occur in auroral arcs (Belon, Romick and Rees, 1966) and this value is in agreement with the value calculated here. Visual auroral forms often have north-south dimensions as small as a kilometer (Chamberlain, 1961) so it seems most likely that the flux observed consisted of electrons.

For most of the examples of i_I increases of small horizontal extent (< 50 km along the satellite path), it was not possible to determine whether they resulted from fluxes or were irregularities in the ambient ionization because simultaneous N_e measurements were not obtained. The occurrence of these small scale increases in i_I was greater during magnetically disturbed conditions.

Comparison of Results with Other Experimental Observations

The results presented in the previous section indicate that N_e and T_e are quite variable at 1000 km within the auroral oval. Other studies of the topside ionosphere have also shown that peaks occur in the electron density in the auroral region (Thomas et al., 1966; Nishida, 1967; Donley, 1968). These studies were mainly concerned with the most pronounced peak, called the polar peak, which occurs during midday and early afternoon, and extends over a latitudinal region much wider than the auroral oval.

From a study of Alouette I data, Nishida (1967) found that N_e peaks exist in the auroral oval at night a finding with which we agree; however we also find that the auroral-oval peaks occur on the dayside but that the nightstide peaks are more pronounced. Andrews and Thomas (1969), also using Alouette I data found N_e peaks and depletions in the oval during winter but not during summer. In contrast our data were obtained in summer and show N_e peaks but they are smaller than those observed by Andrews and Thomas. These differences probably results from the fact that the latitudinal resolution of the electrostatic probe data is significantly greater than that of the topside sounder.

Nishida also found that the nighttime peaks were greatly enhanced during magnetic storms. In this study we find no significant change with magnetic activity. This may arise from the different definitions used for the peak magnitude. Nishida's definition involves the change in N_e from its value during magnetically quiet conditions whereas ours involves the variation along the satellite orbit. Observations by the fixed frequency topside sounder satellite, Explorer 20, indicated logarithmic gradients greater than $60\% \text{ km}^{-1}$ within the auroral zone (Calvert, 1966). These gradients are much larger than those reported here which in most cases were about 0.2% per km. However, such large gradients were not always observed by Explorer 20 and we have considered gradients which extend over tens of kilometers along the satellite path, whereas the large gradient reported by Calvert extended over less than a kilometer. Gradients as large and larger

than those reported by Calvert were observed by the Explorer 22 experiment during an aurora (Findlay et. al., 1969).

4. INTERPRETATION

The properties of the ionosphere at 1000 km altitude result not only from local processes but also from those occurring at other altitudes. Some understanding of the latitudinal variations of N_e and T_e at low and middle latitudes has been gained by Mayr et al. (1967, 1968) in terms of the conservation of energy and density along the closed geomagnetic field lines. At auroral latitudes the situation is rather different from that at lower latitudes as field lines may be open and there are additional processes affecting the ionosphere.

Effects of Precipitating Particles

One of the major additional processes affecting the ionosphere in the auroral oval is the ionization produced by precipitating particles. Hartz and Brice (1967) have shown that there are two zones of precipitating particles. In one of these zones relatively soft electron fluxes precipitate (with energies of the order of a few kev) but the precipitation is very intense, spatially limited, and shows rapid and deep fluctuations. In the other zone the flux is relatively hard (energies of at least 40 kev) and the particle influx is steady and widespread. These zones overlap at night but in daytime the soft electron zone is poleward of the harder precipitation zone. The soft electron zone as derived by Hartz and Brice is coincident with the auroral oval.

The precipitating soft particles lose their energy primarily by ionization of the atmosphere gases. Large numbers of secondary electrons are produced which also produce ionization and heat the electron gas. Most of the ionization is produced at around 150 km or below, and N_e in the F_2 region and above increases as a result of upward diffusion along field lines. When the energy of the secondary electrons has decayed to about 5 ev they become effective in heating the electron gas, increasing its temperature. The thermal electrons lose energy to the positive ions particularly in the upper F region raising the temperature of the ions as well. These increases in the temperature of the plasma increase the scale height and therefore the concentration throughout the topside ionosphere. At 1000 km the increase in T_e and N_e increase the heat losses due to heat conduction and local cooling. Lower in the ionosphere the increase in N_e increases the recombination rate as does the increase in T_e (Thomas and Norton, 1966). If the precipitating flux persists long enough for a steady state to be reached, T_e and N_e increase above their initial values.

However during the dynamic phases, before a steady state is reached and after the flux ceases, N_e and T_e are not necessarily correlated. Hence, although the effect of a precipitating flux is to increase T_e and N_e along a field line, as the satellite passes through the auroral region and crosses field lines along which fluxes of different intensities and duration occur it may not observe a perfect positive correlation between T_e and N_e .

Maxima and minima in N_e and T_e could therefore be produced by latitudinal variations in the precipitating flux. However the minimum values of N_e within the oval are sometimes appreciably smaller than the values just equatorward of the oval (Figure 4) indicating that sometimes there are additional loss processes in the oval region. The increased loss probably results from upward diffusion of ionization due to either evaporation along open field lines (Dessler and Michel, 1966) or the polar wind (Banks and Holzer, 1968). As shown by Block and Fälthammar (1968) ionization fluxes can reduce significantly the electron density at 1000 km.

Effect of Field-Aligned Currents

The transverse magnetic disturbances occurring in the oval region have been interpreted by Cummings and Dessler (1967) to be caused by currents of $\sim 10^{-6}$ amp/m² flowing parallel to the magnetic field direction. Kendall and Pickering (1967) have shown that these currents are too small to affect the electron density in the ionosphere directly. The heating effects of these currents can be estimated in the following way. The joule heating is given by

$$Q_J = j^2 / \sigma_{||} \quad (1)$$

where j is the current density and $\sigma_{||}$ is the electrical conductivity parallel to the field line. In the ionosphere the electron conductivity dominates and is given by (Chapman, 1956)

$$\sigma_{II} = N_e e^2 / M_e \nu_e \quad (2)$$

where e is the electronic charge, M_e the electron mass and ν_e the electron collisions frequency. In the F region and the magnetosphere electron-ion collisions are more important than electron-neutral collisions so that (Banks, 1966)

$$\nu_e = 54 N_e / T_e^{3/2} \text{ sec}^{-1} \quad (3)$$

Currents of $\sim 10^{-6}$ amp m^{-2} could produce the observed magnetic disturbances and substituting this value in equation 1 along with σ_{II} obtained from equations 2 and 3 gives

$$Q_J = .38 \left(\frac{1000}{T_e} \right)^{3/2} \text{ eV cm}^{-3} \text{ sec}^{-1} \quad (4)$$

Below 500 km where local processes are important, $T_e > 1000^\circ\text{K}$ so that joule heating supplies $< 0.38 \text{ eV cm}^{-3} \text{ sec}^{-1}$. This is insignificant compared to heating by secondary electrons which deposit about $100 \text{ eV cm}^{-3} \text{ sec}^{-1}$ in the F region and which in auroral arc can deposit $> 10^4 \text{ eV cm}^{-3} \text{ sec}^{-1}$ (Rees and Walker, 1968).

T_e Within the Oval

For all but two of the passes listed in Table 3, the maximum value of T_e measured in the oval was 3500°K or greater. The largest value observed by this

experiment was 7000°K which occurred simultaneously with a visible aurora (Findlay et al., 1969). Walker and Rees (1968) pointed out that this high temperature could not have resulted at a 1000 km from energetic auroral electron precipitation which heats the ionosphere primarily at lower altitudes. Thus there must have been another heat source on this occasion. In fact for four of the six nighttime cases ($\chi > 90^{\circ}$) listed in Table 3, the maximum value of T_e was at least 3800°K . A comparison with Walker and Rees' calculations for five stable auroral arcs shows that this is somewhat greater than the values obtained by extrapolating their results to 1000 km. It is possible that the electron temperatures are higher because of heating by very low energy electron precipitation (~ 5 ev) in the auroral oval. Another possibility is that there is a heat source in the magnetosphere and that thermal conduction from the magnetosphere causes the high values of T_e (Cole, 1965).

Solar wind electrons have energies of ~ 1 ev associated with their bulk motion and ~ 1 ev of thermal energy (Serbu, 1968). On the dayside the auroral-oval field lines connect to the magnetopause (Fairfield, 1968) so that solar wind particles could be injected along these field lines. These electrons could provide a source of heating at high altitudes for the heat conduction mechanism or alternatively, depending on the accelerating mechanism operative, be the source of a low energy component (~ 5 ev) of precipitating particles which directly heats the ionosphere at 1000 km altitude. The solar wind particles could also be a source of ionization for the enhancements of N_e occurring in the oval.

5. CONCLUSIONS

At 1000 km the ionosphere within the auroral oval is characterized by latitudinal fluctuations in both the electron density and temperature. In this experiment fluctuations were observed in the electron density with dimensions varying from the order of a kilometer to several hundreds of kilometers in latitudinal extent and with enhancements of 10% or greater. The amplitude of the more extensive irregularities (peaks) was greater at night. Similar variations in the electron temperature, with latitudinal extents greater than about 10 kilometers were detected. The degree of correlation between the T_e and N_e fluctuations varies considerably as a result of the dynamic nature of the region.

The maximum value of T_e observed in the oval on some passes is too high to result from energetic auroral particle precipitation suggesting that another heat source exists. One possibility is that very low energy precipitating electrons (~ 5 ev) exist which heat the ionosphere at high altitudes. It is also possible that there is a heat source in the magnetosphere and that the high temperatures result from thermal conduction downwards along the field lines. Either of these mechanisms could be related to solar wind particles injected into the magnetosphere and these particles could also be an additional source of ionization in the oval region.

Transverse magnetic disturbances, potentially ascribable to field-aligned currents were also observed at the satellite height within the region of fluctuating N_e and T_e . However, the direct effect of these currents on the electron density

and temperature are too small to account for the changes observed. Other phenomena which may be associated with these currents (e.g. precipitating particles or ionization fluxes) could cause the variations observed in the ionosphere.

The data also show evidence of intense particle fluxes which are probably low energy electron precipitation events of limited latitudinal extent (tens of kilometers or less).

APPENDIX

Effect of Particle Fluxes on Probe Current

If the satellite passes through a region where energetic particles are precipitating, then a component appears in the probe current due to the energetic particles which strike the probe. This component will be the sum of the currents due to the incident particles and the secondary electrons which leave the probe.

The energy spectrum of the secondary electrons is independent of the incident energy (Schultz and Pomerantz, 1963). It peaks at 2 ev and 90% of the secondaries have energies less than 10 ev. As the secondary electrons leave the probe, they tend to spiral around the magnetic field lines and may return to the probe. However in detecting the fluxes, i_I was measured when the probe was several volts negative with respect to the plasma so that few of the secondaries will be recollected. In addition the probe does not always point directly along the magnetic field lines but may make an angle of up to 6° and this makes it more difficult for a secondary to return to the probe.

The current produced in the probe by a flux of particles can be calculated and we will make the following assumptions.

1. There is a flux of F particles/cm² sec. sterad. with an isotropic pitch angle distribution between 0° and 90° pitch angle.
2. The particles are singly charged.
3. The probe is field-aligned.
4. No secondaries return to the probe.

Then the current collected by a small element of area (Figure 8) is given by

$$dI = e(n \pm 1) F \cdot 2\pi \cdot 2\pi r dI$$

where

n is the number of secondary electrons

r is the probe radius (.275 mm)

$+$ incident particles are protons

$-$ incident particles are electrons

e is the electronic charge

\therefore the total current is given by

$$I = 4eF\pi^2 rL (n \pm 1)$$

where

L is the probe length (23 cm).

Consider first the case of an electron flux striking the probe which is made of stainless steel. The number of secondaries emitted per incident primary varies with the energy of the primaries and Table 4 lists for both Fe and Ni (stainless steel) the energy range over which the yield of secondaries is greater than one. If the yield is less than one, the resultant current will be negative but for yields greater than one, the resultant current is positive because more electrons leave the probe than strike it. Table 4 also shows the maximum yield,

the energy at which it occurs and the average yield over the energy range for which the yield is greater than one. Using the value of the average yield for Ni we find that an average flux of $\sim 5 \times 10^{10}$ particles/cm² sec⁻¹ ster. in the energy range .15-1.75 kev would be needed to produce the change in i_1 shown in Figure 7. Significant fluxes at other energies where the yield of secondaries is less than one would reduce the total current produced by the flux.

In the case of a proton flux the resultant probe current is always positive because both protons striking the probe and electrons leaving the probe constitute a positive current. Few measurements appear to be available for proton bombardment of metals but for some metals the yield of secondaries may be as high as 5 depending on the energy range (Hill et al., 1939). In the case of a proton flux, the change in i_1 in Figure 7 could result from a flux of $\sim 2 \times 10^{10}$ particles cm⁻² sec⁻¹ ster⁻¹ if it is assumed that no secondaries are produced, or from a flux of $\sim 3 \times 10^9$ particles cm⁻² sec⁻¹ ster⁻¹ if it is assumed that 5 secondary electrons are produced for each primary. Therefore, within these uncertainties particle fluxes can be derived from probe data. However, in the case of the Explorer 22 probe experiment, any large scale study of fluxes using this method would be very difficult because N_e is not measured continuously.

ACKNOWLEDGMENTS

We are indebted to George Carignan and Tuck Bin Lee of the University of Michigan for their efforts in the design and implementation of the probe instrument and to the members of the APL tracking station crew for their efforts

in obtaining these special passes. We are also grateful to Pierre Amiot for his aid in analyzing the data and W. E. Radford (APL), E. Marshall (API), J. C. G. Walker (Yale University) and L. H. Brace (GSFC) for valuable discussions. Part of this work was supported by the Naval Ordnance Systems Command, U.S. Dept. of the Navy Under contract number NOW 62-0604-C.

REFERENCES

Akasofu, S.-I., The auroral oval, the auroral substorm, and their relations with the internal structure of the magnetosphere. Planetary Space Sci., 14, 587, 1966.

Akasofu, S.-I., and S. Chapman, The lower limit of latitude (U. S. sector) of northern quiet auroral arcs, and its relation to D st (H), J. Atmospheric Terrest. Phys., 25, 9-12, 1963.

Akasofu, S.-I., S. Chapman and C. I. Meng, The polar electrojet, J. Atmospheric Terrest. Phys., 27, 1275-1305, 1965.

Andrews, M. K., and J. O. Thomas, Electron density distribution above the winter pole, Nature, 221, 223, 1969.

Banks, P. M., and T. E. Holzer, The Polar Wind, J. Geophys. Res. 73, 6846, 1968.

Banks, P. M., Collision frequencies and energy transfer. Electrons, Planet. Space Sci., 11, 1055, 1966.

Bates, H. F., Latitude of the dayside aurora, J. Geophys. Res., 71, 3629-3633, 1966.

Bates, H. F., A. E. Belon, G. J. Romick, and W. J. Stringer, On the correlation of optical and radio auroras, J. Atmospheric Terrest. Phys., 28, 439-446, 1966.

Belon, A. E., G. J. Romick and M. H. Rees, The energy spectrum of primary auroral electrons determined from auroral luminosity profiles, Planet. Space Sci., 14, 597, 1966.

Block, L. P., and C.-G Falthammar, Effects of field-aligned currents on the structure of the ionosphere, J. Geophys. Res. 73, 4807, 1968.

Boström, R., Auroral Electric Fields, Aurora and Airglow, Reinhold Publishing Corporation, 293, 1967.

Brace, L. H., K. K. Mahajan and M. G. Mayr, Polar peak of electron concentration (presented at URSI meeting in Washington, April, 1969).

Brace, L. H., H. G. Mayr and B. M. Reddy, The early effects of increasing solar activity upon the temperature and density of the 1000-kilometer ionosphere, J. Geophys. Res., 73, 1607, 1968.

Brace, L. H., and B. M. Reddy, Early electrostatic probe results from Explorer 22, J. Geophys. Res., 70, 5783, 1965a.

Brace, L. H., and B. M. Reddy, Latitudinal variations of electron temperature and concentration from satellite probes, NASA X-651-65-190, 1965b.

Brace, L. H., B. M. Reddy, and H. G. Mayr, Global behavior of the ionosphere at 1000-kilometer altitude, J. Geophys. Res., 72, 265, 1967.

Brace, L. H., N. W. Spencer, and A. Dalgarno, Detailed behavior of the mid-latitude F region from Explorer 17 satellite, Planetary Space Sci., 13, 647, 1965.

Calvert, W., Steep horizontal electron-density gradients in the Topside F layer, J. Geophys. Res., 71, 3665, 1966.

Calvert, W., and T. E. Van Zandt, Fixed-frequency observations of plasma resonances in the topside ionosphere, J. Geophys. Res. 71, 1799, 1966.

Chamberlain, J. W., Physics of the aurora and airglow, Academic Press, New York, 1961.

Chapman, S., The electrical conductivity of the ionosphere: a review, Nuovo Cimento Supp., 4, 1385, 1956.

Cole, K. D., Stable auroral red arcs, sinks for energy of D_{st} main phase, J. Geophys. Res., 70, 1689, 1965.

Cummings, W. D., and A. J. Dessler, Field-aligned currents in the magnetosphere, J. Geophys. Res., 72, 1007, 1967.

Dessler, A. J., and F. C. Michel, Plasma in the geomagnetic tail, J. Geophys. Res., 71, 1421, 1966.

Donley, J. L. Observations of the polar ionosphere in the altitude range 2000 to 3000 km by means of satellite borne electron traps, Space Research, 8, 381, 1968.

Dyson, P. L., Direct measurement of the size and amplitude of irregularities in the topside ionosphere (NASA X-621-69-57) 1969.

Eather, R. H., Auroral proton precipitation and hydrogen emissions, Rev. Geophys., 5, 207, 1967.

Fairfield, D. H., Average Magnetic Field Configuration of the Outer Magnetosphere, J. Geophys. Res., 73, 7329, 1968.

Feldstein, Y. I., Some problems concerning the morphology of auroras and magnetic disturbances at high latitudes, Geomagnetism and Aeronomy, 3, 183, 1963.

Feldstein, Ya. I., Peculiarities in the auroral distribution and magnetic disturbance distribution in high latitudes caused by the asymmetrical form of the magnetosphere, Planetary Space Sci., 14, 121-130, 1966.

Findlay, J. A., P. L. Dyson, L. H. Brace, A. J. Zmuda, and W. E. Radford, Observations of electron temperature and density at 1000 kilometers during the May 25-26, 1967 auroral sub-storm. (To be published in J. Geophys. Res., 1969.)

Frank, L. A., J. A. Van Allen, and J. D. Craven, Large diurnal variations of geomagnetically trapped and of precipitated electrons observed at low altitudes, J. Geophys. Res., 69, 3155-3167, 1964.

Hartz, T. R., and N. M. Brice, The general pattern of auroral particle precipitation, Planetary Space Sci., 15, 301, 1967.

Heuring, F. T., A. J. Zmuda, and J. C. Armstrong. Transverse magnetic disturbances at 1100 km in the auroral oval (Abstract). Trans. Am. Geophys. Union, 49, 738, 1968.

Hill, A. G., W. W. Beuchner, J. S. Clark and J. B. Fisk, The emission of secondary electrons under high energy positive ion bombardment, Phys. Rev., 55, 463, 1939.

Kendall, P. C., and W. M. Pickering, Magnetoplasma diffusion at F_2 -region altitudes. Planetary Space Sci., 15, 825, 1967.

Lund, D. S., R. D. Hunsucker, H. F. Bates, and W. B. Murcray, Electron number densities in auroral irregularities: Comparison of backscatter and satellite data, J. Geophys. Res., 72, 1053, 1967.

Mahajan, K. K., and L. H. Brace, Global Observations on the Thermal balance of the nighttime protonosphere, NASA-X-621-68-506, 1968.

Mayr, H. G., L. H. Brace, and W. Crevier, The latitudinal temperature structure of the topside ionosphere. Submitted to J. Geophys. Res., 1968.

Mayr, H. G., L. H. Brace, and G. S. Dunham, Ion composition and temperature in the topside ionosphere, J. Geophys. Res., 73, 1607, 1968.

McDiarmid, I. B., and J. R. Burrows, Diurnal intensity variations in the outer radiation zone at 1000 km, Can. J. Phys., 42, 1135-1148, 1964.

Mott-Smith, H. M., and I. Langmuir, The theory of collectors in gaseous discharges, Phys. Rev., 28, 727, 1926.

Muldrew, D. B., F-layer ionization troughs deduced from Alouette Data, J. Geophys. Res., 70, 2635, 1965.

Nishida, A., Average structure and storm-time change of the polar topside ionosphere at sunspot minimum, J. Geophys. Res., 72, 6051, 1967.

O'Brien, B. J., Lifetimes of outer-zone electrons and their precipitation into the atmosphere, J. Geophys. Res., 67, 3687-3706, 1962.

O'Brien, B. J., A large diurnal variation of the geomagnetically trapped radiation, J. Geophys. Res., 68, 989-995, 1963.

Piddington, J. H., The morphology of auroral precipitation, Planetary Space Sci., 13, 565-577, 1965.

Rees, M. H., and J. C. G. Walker, Ion and electron heating by auroral electric fields, Am. Geophys., 24, 193, 1968.

Serbu, G. P., Explorer 35 Measurements of low energy plasma in lunar orbit,
J. Geophys. Res., 74, 372, 1969.

Schield, M. A., Configuration of geomagnetic field lines above the auroral zones,
Ph.D. Thesis, Rice University, Houston, Texas, 1968.

Schield, M. A., J. W. Freeman, and A.J. Dessler, A source of field-aligned
currents at auroral latitudes. J. Geophys. Res., 74, 247, 1969.

Shultz, A. A., and M. A. Pomerantz, Secondary electron emission produced by
relativistic primary electrons, Phys. Rev., 130, 2135, 1963.

Spencer, N. W., L. H. Brace, G. R. Carignan, D. R. Taeusch, and H. Niemann,
Electron and molecular nitrogen temperature and density in the thermos-
phere, J. Geophys. Res., 70, 2665, 1965.

Taylor, H. A., Jr., H. C. Brinton, M. W. Pharo, III, and N. K. Rahman, Thermal
ions in the exosphere: Evidence of solar and geomagnetic control, J.
Geophys. Res., 73, 5521, 1968.

Thomas, L., and R. B. Norton, Possible importance of internal excitation in
ion-molecule reactions in the F region, J. Geophys. Res., 71, 227, 1966.

Thomas, J. O., M. J. Rycroft, L. Colin, and K. L. Chan, The topside ionosphere,
2, Experimental results from the Alouette I satellite, in Electron Density
Profiles in Ionosphere and Exosphere, pp. 322, North-Holland Publishing
Company, Amsterdam, 1966.

Walker, J. C. G., and M. H. Rees, Ionospheric Electron Densities and Tempera-
tures in Aurora, Planetary Space Sci., 16, 459, 1968.

Williams, D. J., and G. D. Mead, Nightside magnetosphere configuration as obtained from trapped electrons at 1100 km, J. Geophys. Res., 70, 3017-3029, 1965.

Williams, D. J., and W. F. Palmer, Distortions in the radiation cavity as measured by an 1100-kilometer polar orbiting satellite, J. Geophys. Res., 70, 557-567, 1965.

Zmuda, A. J., J. H. Martin, and F. T. Heuring, Transverse magnetic disturbances at 1100 km in the Auroral region, J. Geophys. Res., 71, 5033, 1966.

Zmuda, A. J. F. T. Heuring, and J. H. Martin, Dayside magnetic disturbances at 1100 kilometers in the auroral oval, J. Geophys. Res., 72, 1115, 1967.

Table 1

Number of cases in which $(N_e)_{\max}$, $(N_e)_{\min}$, and the maximum logarithmic N_e gradient occur inside and outside of magnetic disturbance region.

	$(N_e)_{\max}$	$(N_e)_{\min}$	$(1/N_e)(dN_e/dx)_{\max}$
Number in ΔB region	20	15	17
Number outside ΔB region	9	14	12

Table 2

Summary of the values of $(N_e)_{\max}$, $(N_e)_{\min}$, and the maximum of the logarithmic N_e gradient

Ionospheric quantity	Range of ionospheric quantity		
	In cases where a ΔB region was observed		In cases where no ΔB was observed
	in ΔB region	outside ΔB region	
$(N_e)_{\max}$ (electrons/cm ³)	$(2.1-4.0) \cdot 10^4$	$(2.3-3.8) \cdot 10^4$	$(2.5-4.0) \cdot 10^4$
$(N_e)_{\min}$ (electrons/cm ³)	$(1.9-3.2) \cdot 10^4$	$(1.9-3.5) \cdot 10^4$	$(2.0-3.6) \cdot 10^4$
$1/N_e (dN_e/dx)_{\max}$ (per km)	$(0.5-10) \cdot 10^{-3}$	$(0.9-9) \cdot 10^{-3}$	$(0.1-10) \cdot 10^{-3}$

Table 3
Summary of electron temperature data

Day	UT	Zenith Angle of Sun at 65°A	T_e max (°K)	T_e min (°K)	Background T_e (°K)	$\left(\frac{dT_e}{dx}\right)$ oval (degrees/km)	$\left(\frac{dT_e}{dx}\right)$ Background (degrees/km)
122	0507	114	4200	2000	2300*	34	<1.0*
123	0349	113	4400	2200	—	23	—
145	0134	97	3000	2300	2500	14	2.5
146	0202	95	7000	2600	3000*	52	1.5
	1115	66	5500	2800	3400	26	4.5
147	0044	94	3500	3000	3000	13	4
	0231	94	3800	3000	3000	13	2.5
	1142	66	3200	2900	3000	2.5	1.5
148	1210	68	4200	3000	3500	25	3.5
179	2030	52	3500	2800	3000	23	2.5
180	2058	51	3700	2700	3250	10	2.5

Table 4
 Summary of secondary electron data for bombardment
 of nickel and iron by electrons

Metal	Energy range in kev for which yield is greater than 1	Maximum of secondaries	Energy in kev for which yield is max.	Ave. yield over energy range in column 2
Ni	0.15-1.75	1.35	0.55	1.20
Fe	0.12-1.40	1.3	(0.40)	1.16

EXPLORER XXII
VOLT-AMPERE CHARACTERISTICS
HIGH CURRENT CHANNEL LOW CURRENT CHANNEL

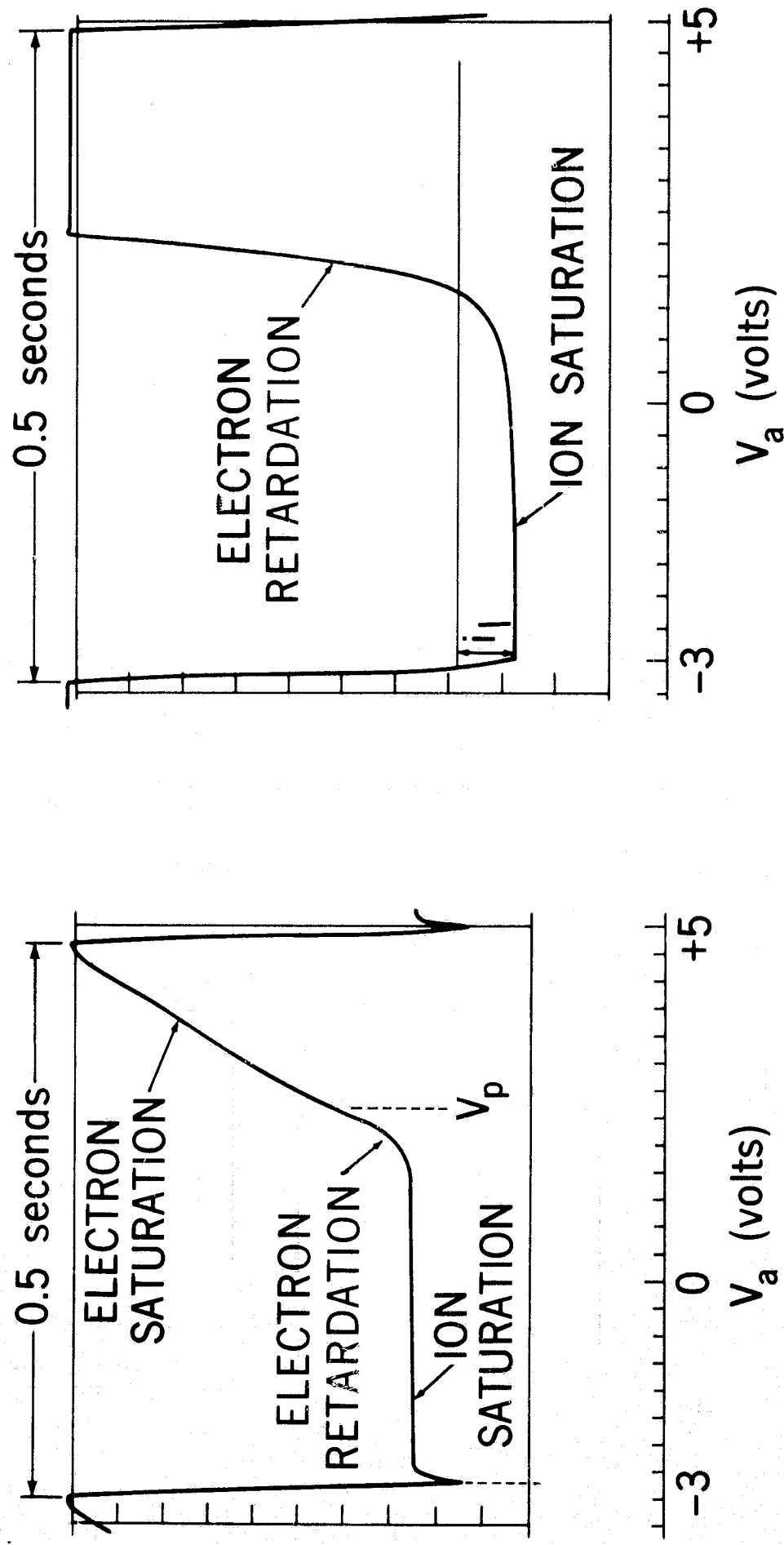


Figure 1—Typical volt-ampere characteristics from the Explorer 22 electrostatic probe experiment

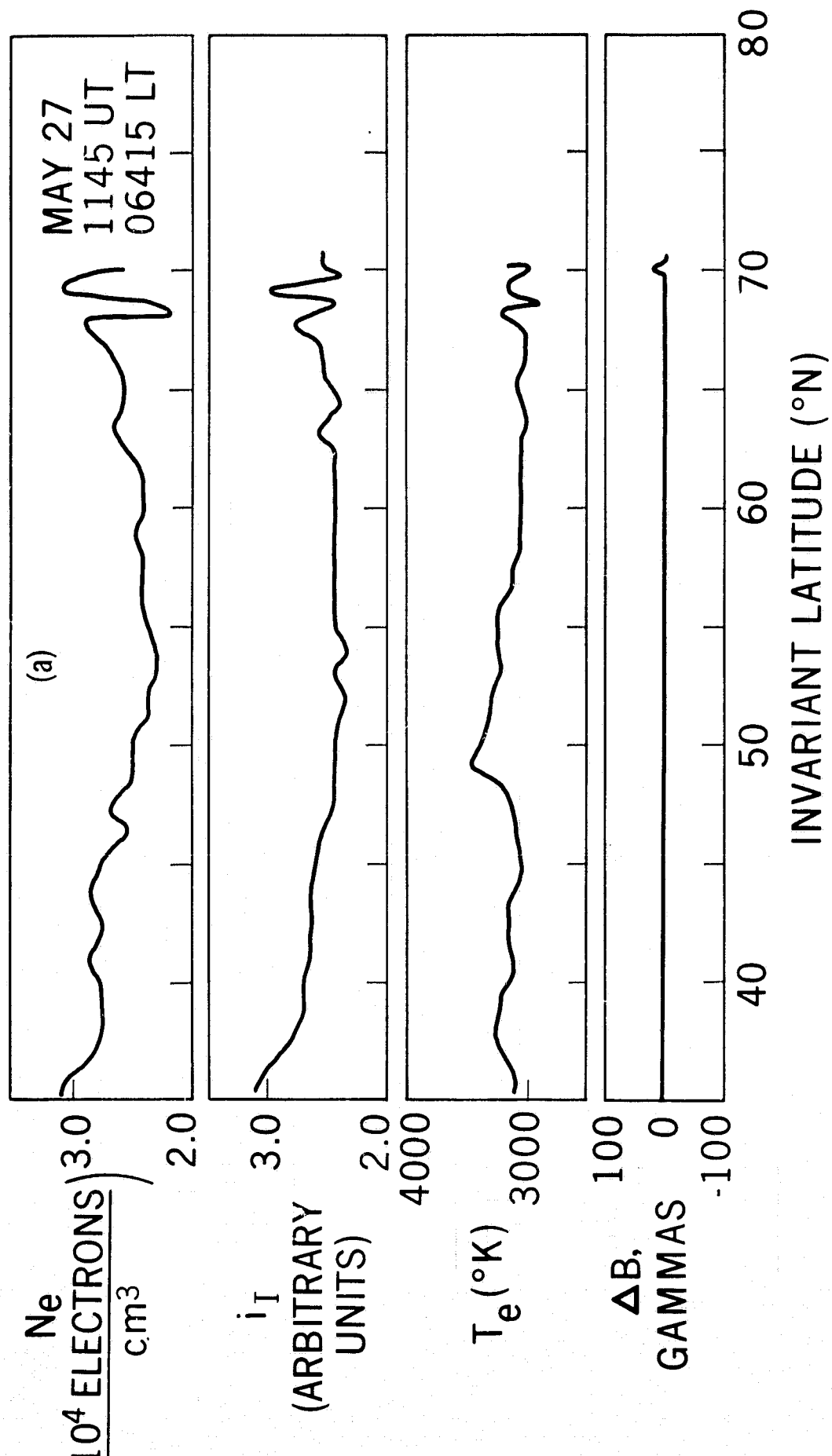


Figure 2a—Typical plots of N_e , T_e , and i , along the orbital path.
The magnetic variations are also shown.

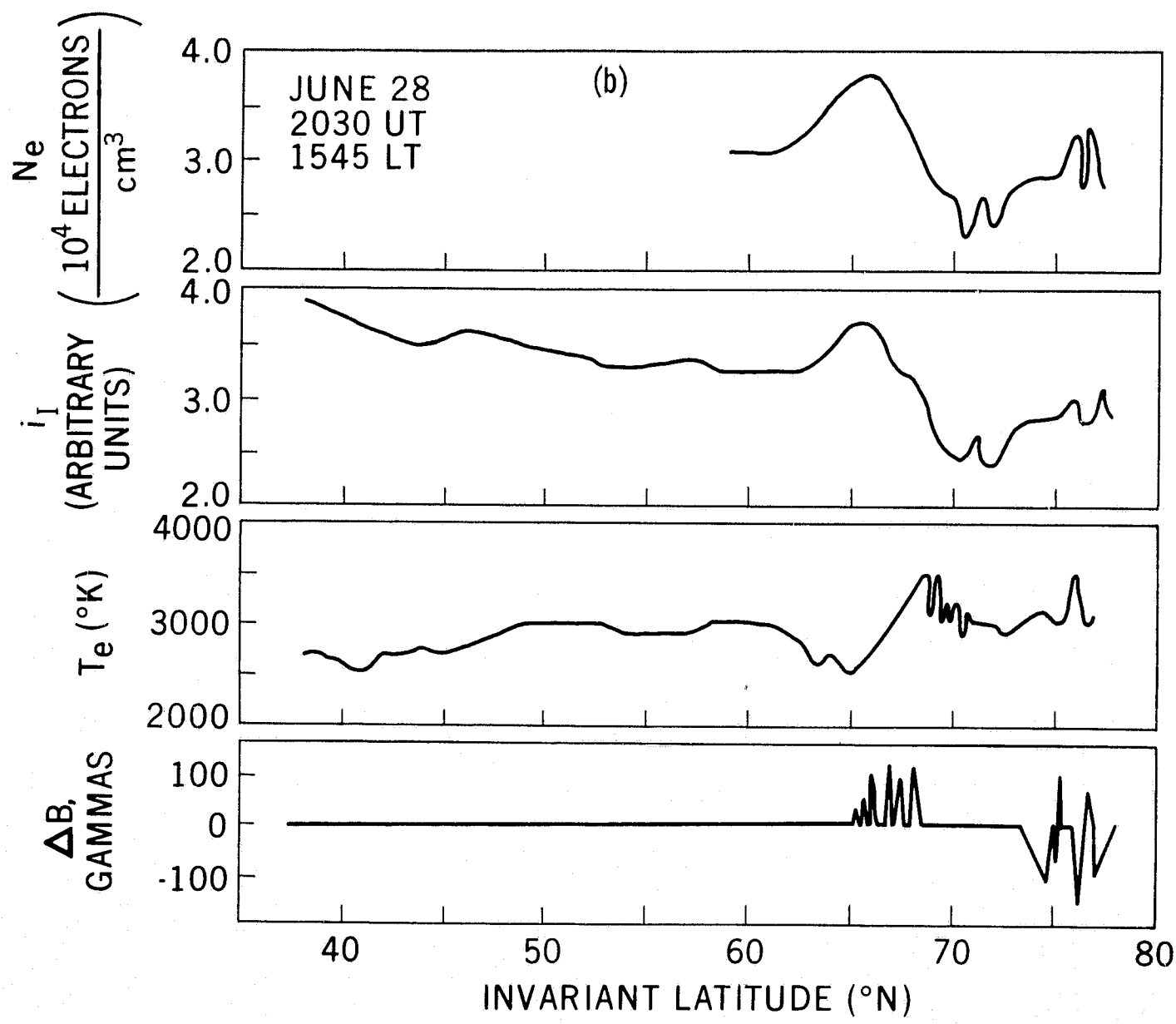


Figure 2b—Typical plots of N_e , T_e , and i_1 along the orbital path.
The magnetic variations are also shown.

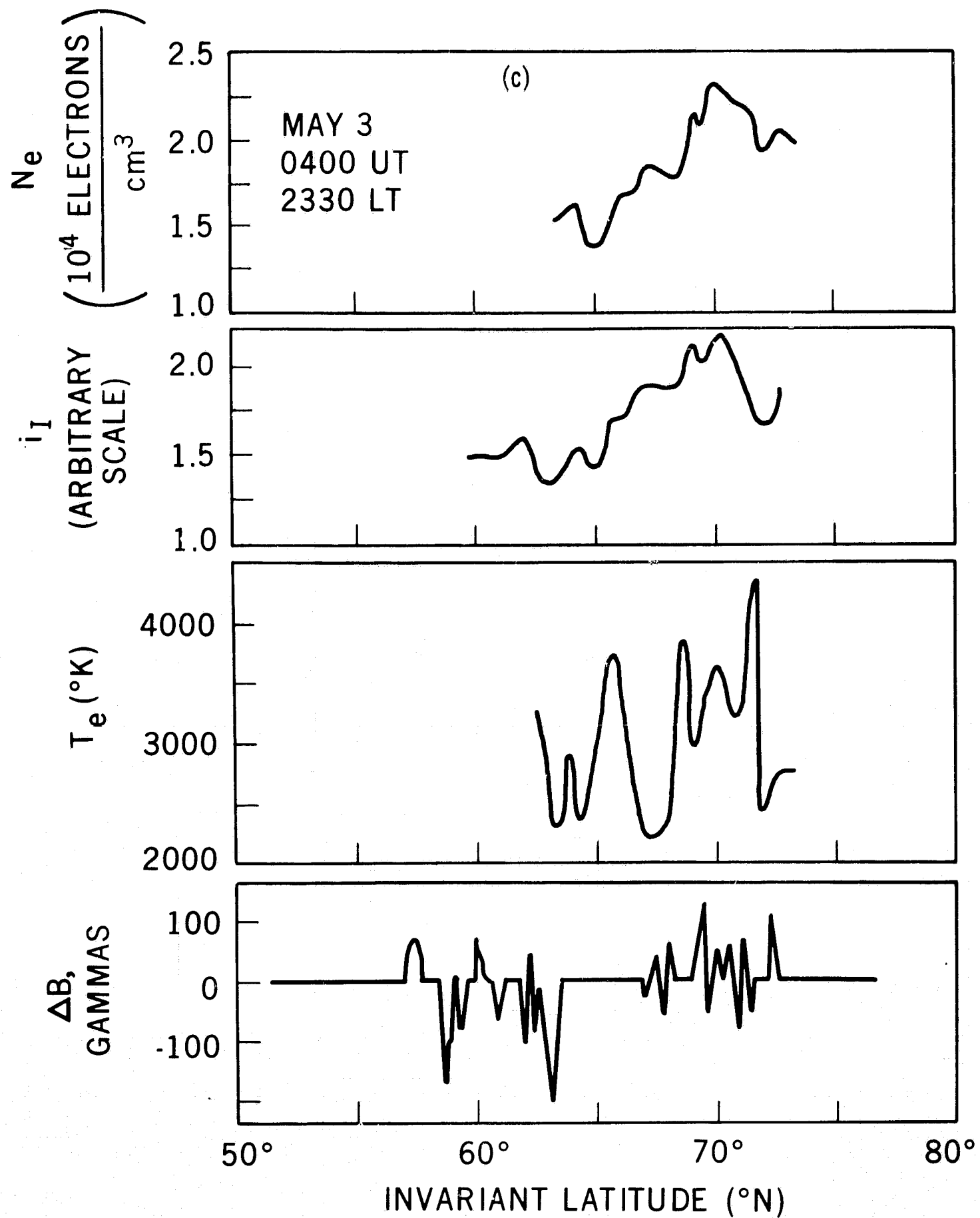


Figure 2c—Typical plots of N_e , T_e , and i_I along the orbital path.
The magnetic variations are also shown.

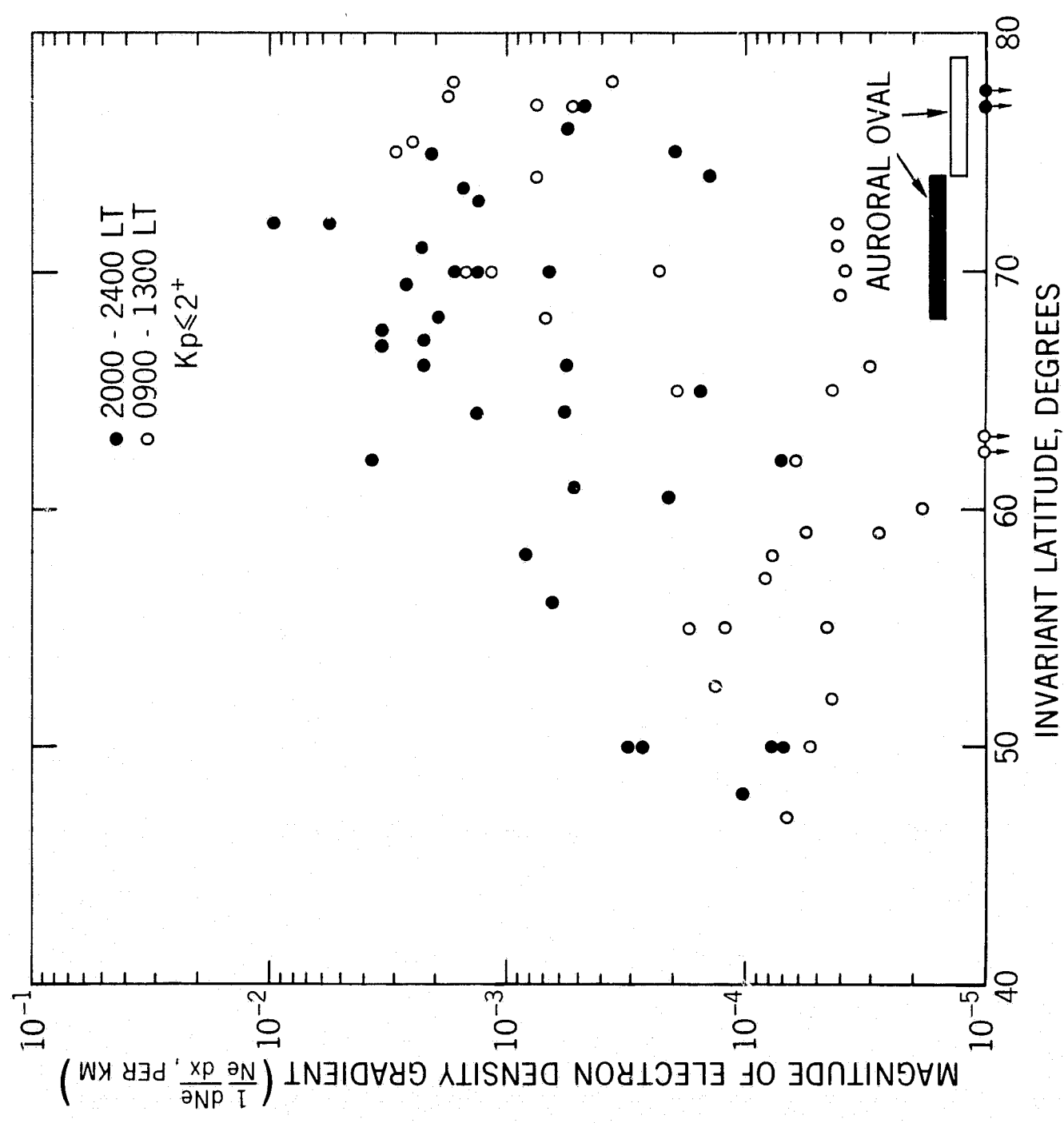


Figure 3—Horizontal electron density gradient as a function of invariant latitude.

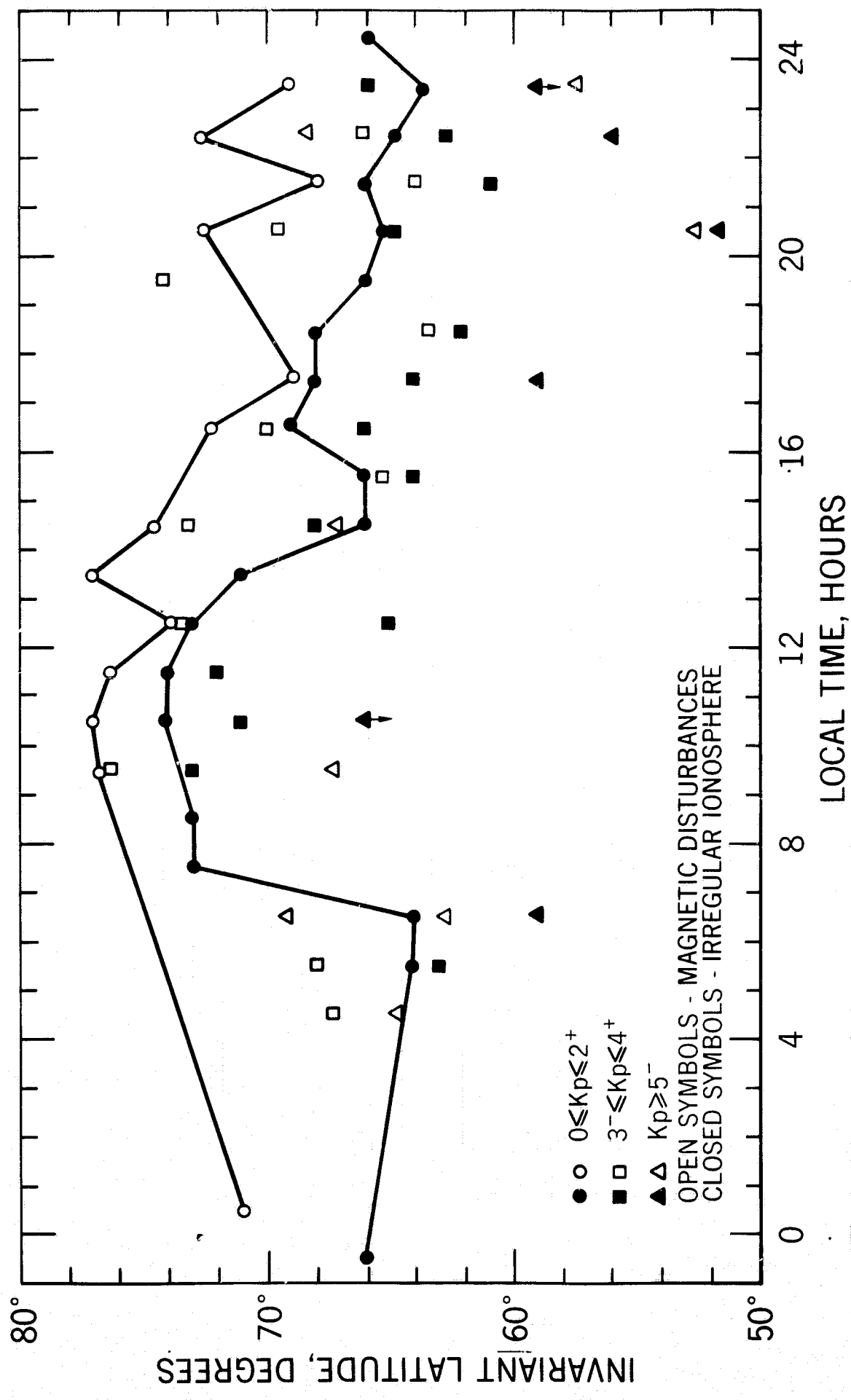


Figure 4—The relation between the auroral oval and the equatorward boundary of the irregular ionosphere.
 (○, □, △, magnetic disturbances, ●, ■, ▲, equatorward boundary of irregular ionosphere.)

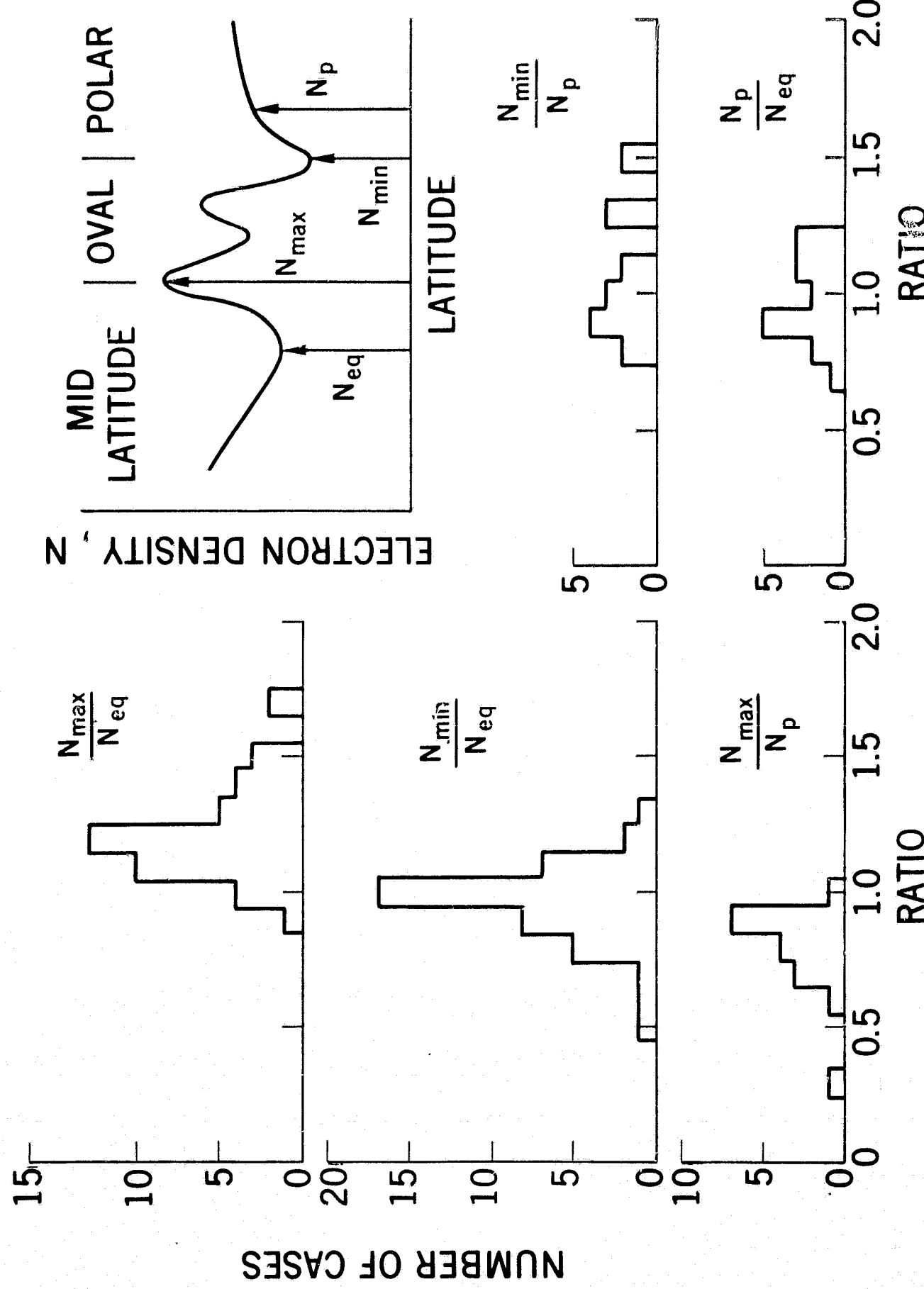


Figure 5—Histograms of the ratio of the electron densities measured at the different locations shown in the upper right diagram.

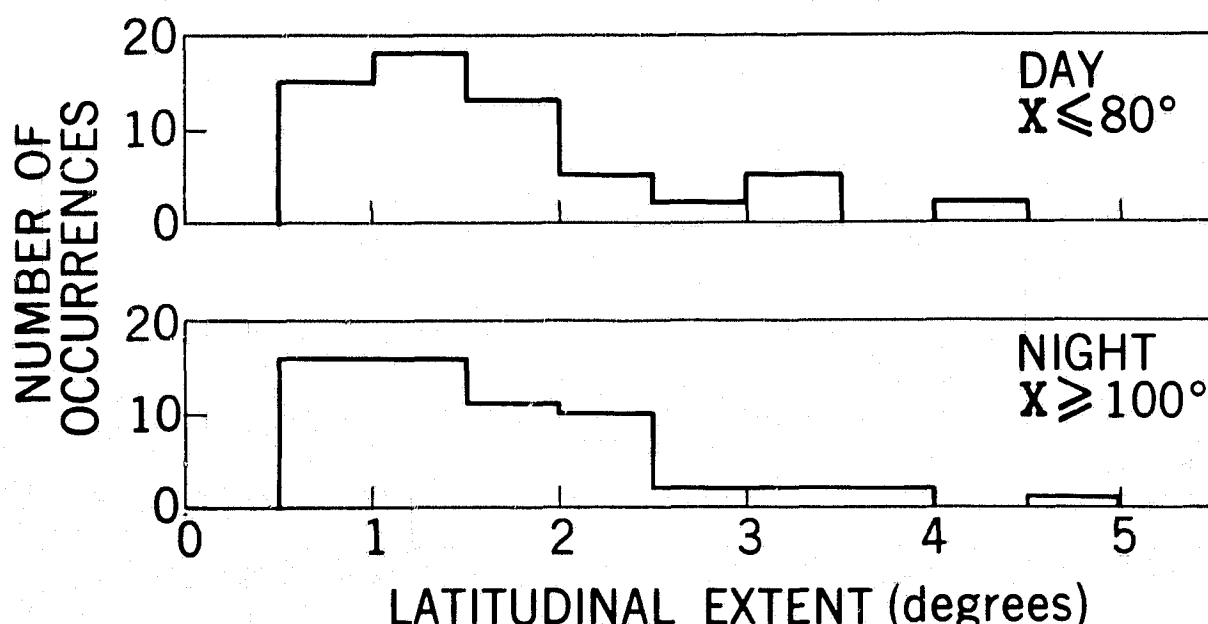
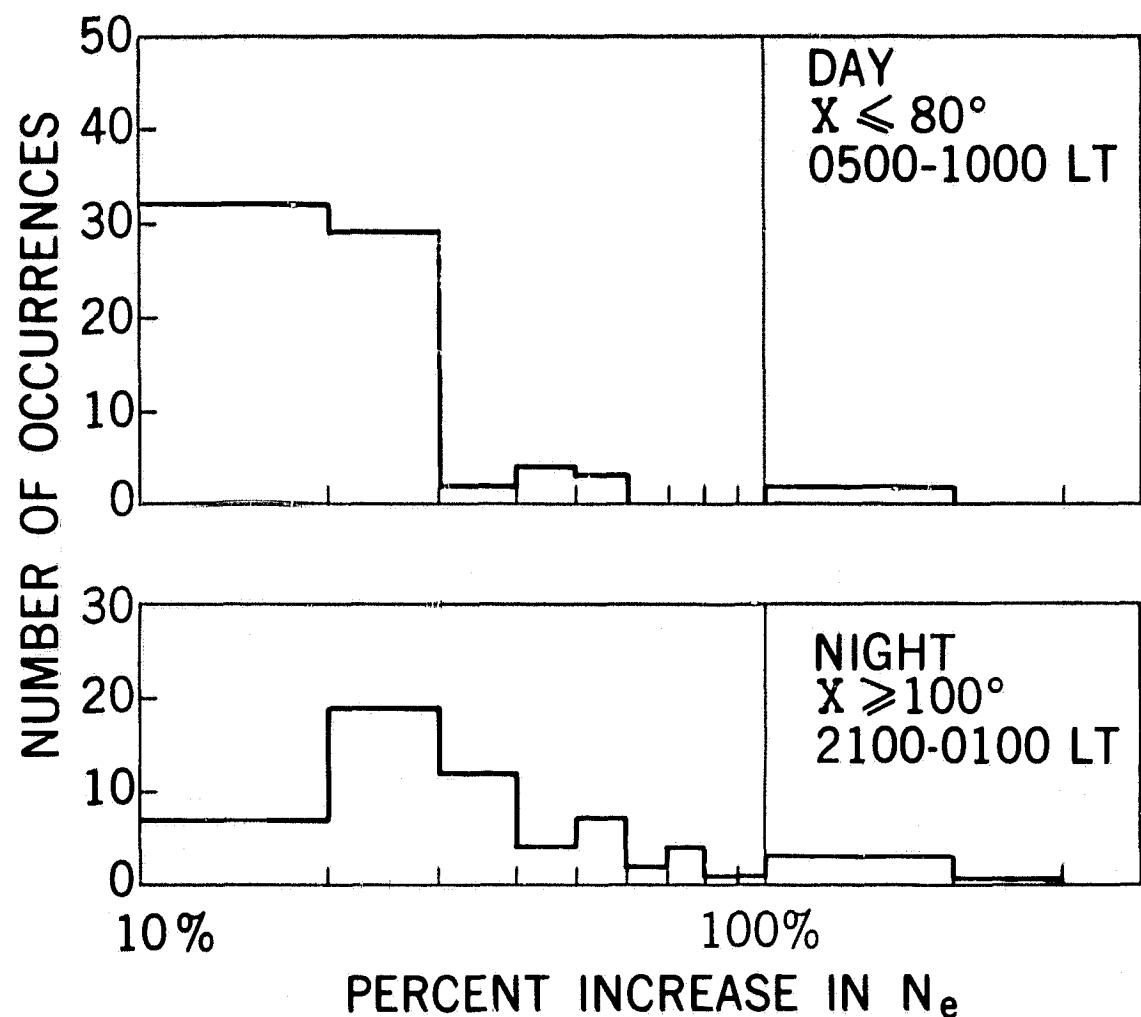


Figure 6—Plots of (a) the magnitude and (b) latitudinal extent of N_e peaks.

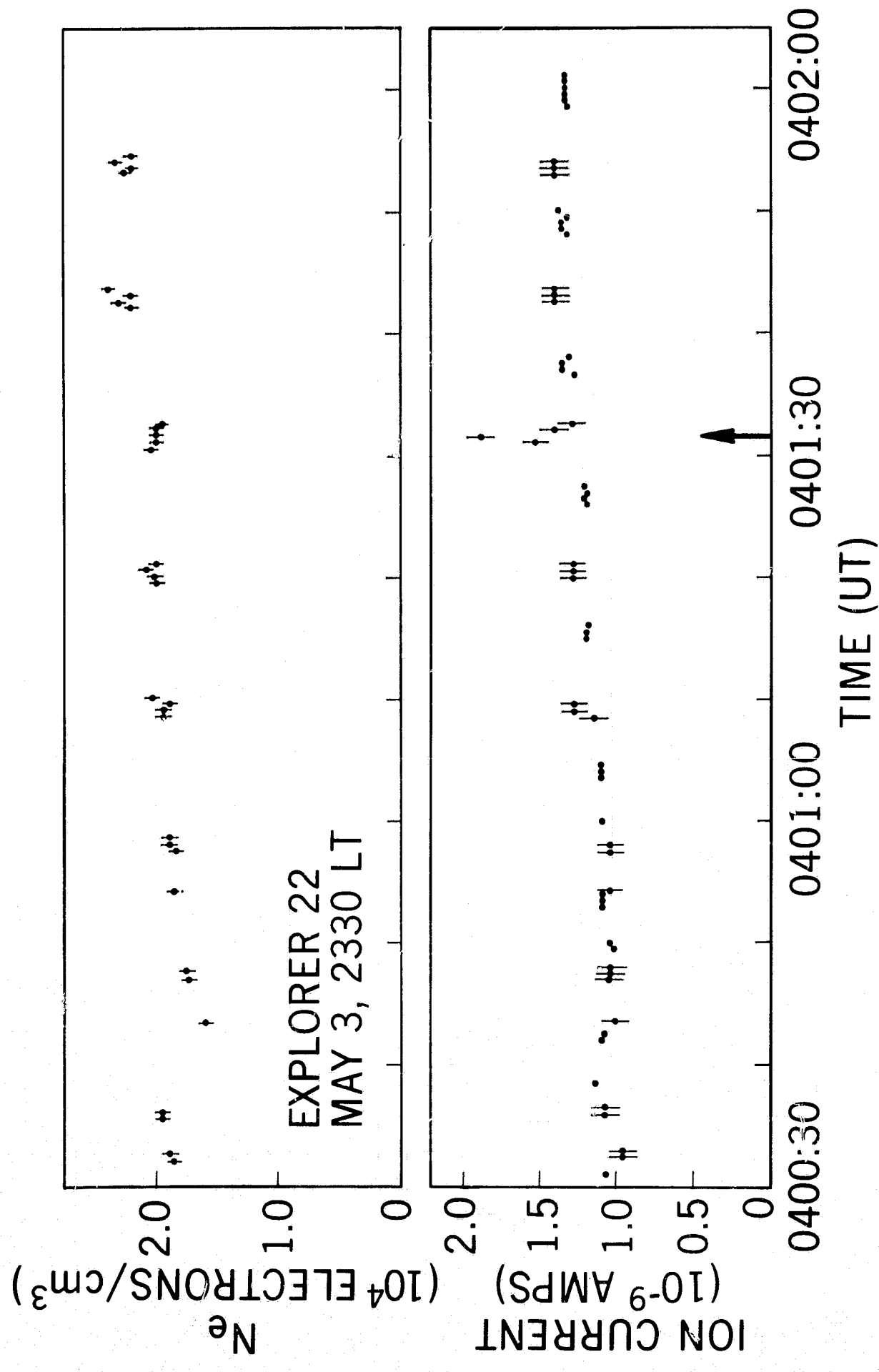


Figure 7—A section of the data from a pass on May 3 showing a large increase in i_i produced by a flux of energetic particles. The ion current zero has been arbitrarily chosen.

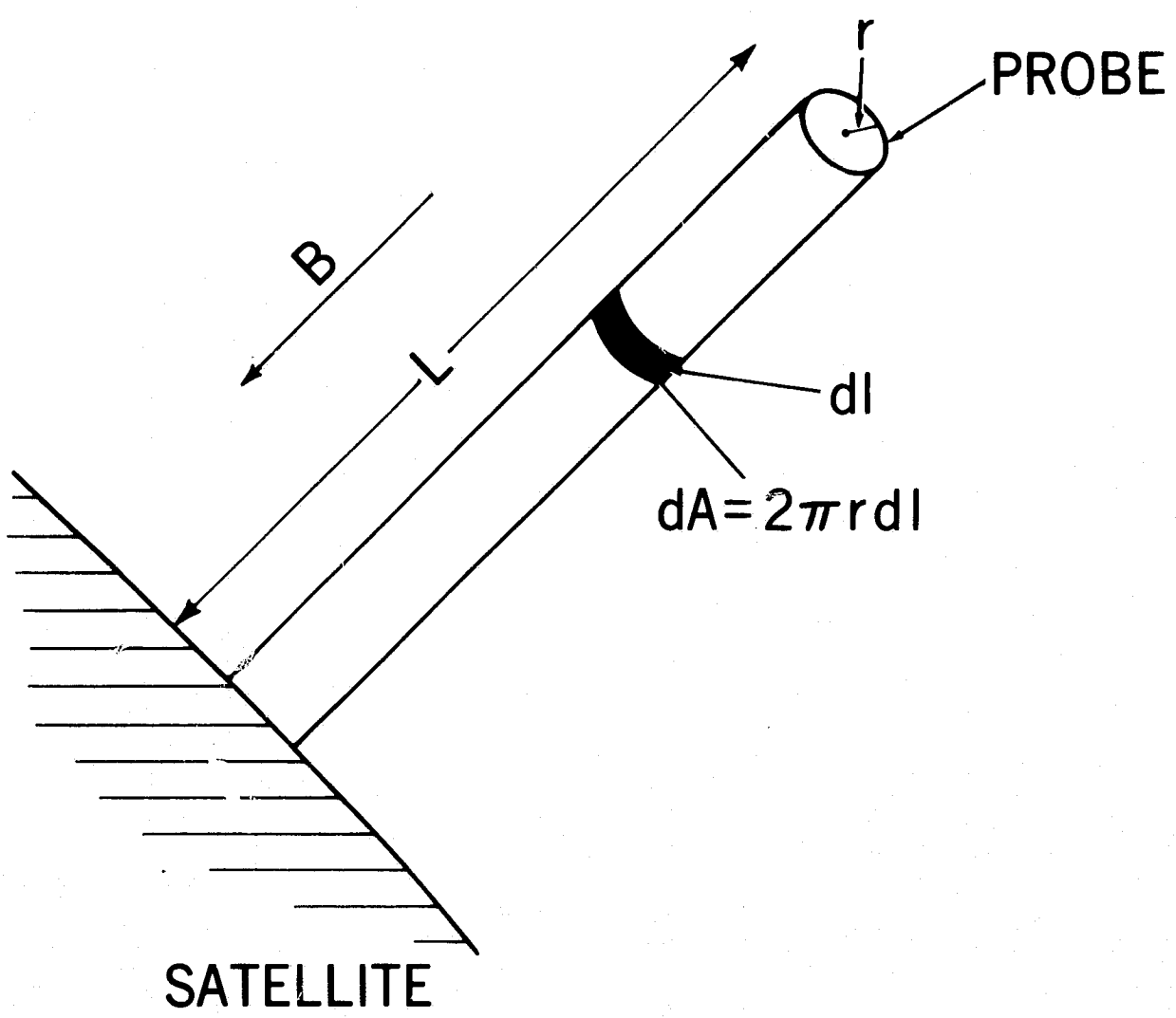


Figure A1—Schematic diagram of the electrostatic probe.